PASSIVE NEAR-FIELD SOURCE LOCALIZATION BASED ON SPATIAL-TEMPORAL STRUCTURE

Y. Wu

Wuhan Institute of Technology
Wuhan 430073, China

H. C. So

Department of Electronic Engineering
City University of Hong Kong
Kowloon, Hong Kong, China

C. Hou

Institute of Acoustics
Chinese Academy of Sciences
Beijing 100080, China

Abstract—A new subspace method based on spatial-temporal structure is presented for estimation of directions-of-arrival (DOA's) and ranges of multiple near-field sources impinging on an array of sensors. The arrival angle and range parameters are directly given by the eigenvalues of a set of constructed matrices and the computational complexity of the proposed method is lower than those of several available methods which do not require search operation. Simulation results show that the proposed method outperforms an ESPRIT-like method.

1. INTRODUCTION

In array signal processing, many methods for estimation of direction-of-arrival (DOA) of far-field source impinging on an array of sensors have been developed [1], such as MUSIC and ESPRIT. Most of these methods assume that the received sources are located relatively far from the array and hence the wavefronts from the sources can be

---

Corresponding author: Y. Wu (ytwu@sina.com).

regarded as plane waves. With this assumption, each source location can be characterized by a single DOA [1]. When the source is close to the array which corresponds to the near-field scenario, the plane wave assumption is no longer valid. The near-field sources must be characterized by spherical wavefronts at the array aperture and need to be localized by both range and DOA [2–5]. Note that the near-field situation is common in applications for sonar [2], seismic exploration [3] and electronic surveillance [8], etc.

Since the available methods based on the far-field assumption cannot be directly applied to the case of near-field, in recent years, the problem of near-field source localization has attracted much attention in the literature [2–11]. The maximum likelihood estimator is proposed in [2] and the resulting estimates have optimal statistical properties, but it requires a multidimensional search and is highly non-linear. Huang et al. [4] and Jeffers et al. [5] have extended the conventional 1-D MUSIC method to 2-D for joint range and DOA estimation. However, the 2-D MUSIC technique of [4] requires an exhaustive 2-D search which corresponds to a high computation cost. Instead of 2-D search, [5] is explicitly shown to involve two 1-D searches in an alternating maximization scheme which can be implemented in a computationally efficient manner. Starer and Nehorai [6] have proposed a path-following algorithm in which the peaks of the 2-D MUSIC spectrum are found by following the paths. This path-following algorithm requires fewer computations than that of the 2-D MUSIC approach because it searches the 1-D paths to estimate the source location. However, the required path calculations correspond to a bulky computational burden. In order to reduce the computational complexity of [6], a modified path-following algorithm using a known algebraic path has been devised in [7]. In addition, Lee et al. [8] have used the conventional far-field beamforming output to initialize a 3-D search and thus the computational burden is reduced to some extent. Weiss and Friedlander [9] have developed a method for DOA estimation at a given trial range value using a polynomial rooting method which makes the 2-D search simpler. To avoid the multidimensional search, Challa and Shamsunder [10] have developed a total least squares ESPRIT-like algorithm based on the fourth-order cumulant. Unfortunately, it still requires large amount of computations to construct a high-dimension cumulant matrices as well as a large number of snapshots for accurate cumulant estimation and is applicable only for non-Gaussian sources. More recently, a weighted linear prediction method for near-field source localization is presented in [11, 12]. Nevertheless, a set of complex optimization calculations and weighting matrix inverses are required to improve the estimation

accuracy.

In this paper, a spatial-temporal structure based method for joint DOA and range estimation of near-field sources is presented. The motivation for using the spatial-temporal structure of spatial correlation sequences is to reduce the effect of observed noise as well as to achieve performance improvement in the case of limited data snapshots by constructing the so-called "pseudo-snapshots" [14, 15]. The proposed method uses only second-order statistics and is suitable for both Gaussian and non-Gaussian signal sources. A closed-form estimation of both DOA and range is provided through a subspace method. The rest of the paper is organized as follows. Section 2 describes the data model for the near-field source localization and the problem formulation. The proposed algorithm is developed in Section 3. Finally, simulation results are provided in Section 4, followed by a conclusion in Section 5.

2. PROBLEM FORMULATION

We consider the narrow-band model for array processing of near-field sources where there are P narrow-band sources received by a uniform linear array of $n = 2N + 1$ sensors with inter-element spacing d. The array configuration is shown in Figure 1. For unique estimation, we require $d \leq \lambda/4$ [10] where λ denotes the wavelength of the source wavefronts and $N > P$. The output of the mth sensor can be approximated as [2–11]:

$$x_m(t) = \sum_{i=1}^{P} s_i(t)e^{j(\omega_i m + \phi_i m^2)} + n_m(t), \quad t = 1, 2, \ldots, M \qquad (1)$$

for $m = -N, \ldots, 0, 1, \ldots, N$. It is assumed that P is known *a priori* and the P sources $\{s_1(t), \ldots, s_P(t)\}$ are statistically independent of each other while the additive noise component $n_m(t)$ is a zero-mean white Gaussian process and is independent of the source signals. Here we let the sensor $m = 0$ be the phase reference point, which is also the origin of our coordinate system. The parameters ω_i and ϕ_i are functions of the azimuth angle θ_i and range r_i of the ith source, and they are expressed as

$$\omega_i = \frac{-2\pi}{\lambda} d \sin(\theta_i) \qquad \text{and} \qquad \phi_i = \frac{d^2 \pi}{\lambda r_i} \cos^2(\theta_i) \qquad (2)$$

The goal is to estimate the parameters $\{\theta_1, \ldots, \theta_P, r_1, \ldots, r_P\}$ of the P sources from the received array data $\{x_{-N}(t), \ldots, x_N(t)\}$.
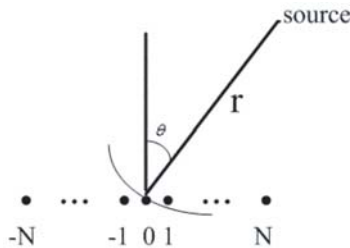
Figure 1. Configuration of uniform linear array.

3. THE PROPOSED ALGORITHM

The proposed method can be divided into two steps and uses only second-order statistics of the array output. The first step is a signal pre-processing which consists of the computation of some properly chosen spatial correlation sequences of the observed signal. These correlation coefficients are shown to be superimposed exponential sequences and their frequencies are linear functions of angles and ranges of the source signals.

The second step is to transform the cross-correlated spatial sequences of the observed signal from 1-D space domain to 2-D space-time domain and then use a subspace rotation invariance technique to obtain the estimates of ω_i and ϕ_i.

Under the assumption of spatial-temporal white Gaussian noise, the correlation sequences for $\{x_m(t)\}$ are:

$$r_{(-l,l)}(\tau) = \sum_{i=1}^{P} r_{s_i s_i}(\tau) e^{-2j\omega_i l} + \sigma^2 \delta(l+\tau) \tag{3}$$

$$r_{(-l-1,l)}(\tau) = \sum_{i=1}^{P} r_{s_i s_i}(\tau) e^{-j(\omega_i - \phi_i)(2l+1)} \tag{4}$$

$$r_{(-l+1,l)}(\tau) = \sum_{i=1}^{P} r_{s_i s_i}(\tau) e^{-j(\omega_i + \phi_i)(2l-1)} \tag{5}$$

where

$$r_{(k,l)}(\tau) = E\{x_k(t+\tau/2)x_l^*(t-\tau/2)\}, \ \ k = -N, \ldots, 0, \ l = 0, 1, \ldots, N \tag{6}$$

and

$$r_{s_i s_i}(\tau) = E\{s_i(t+\tau/2)s_i^*(t-\tau/2)\} \tag{7}$$

is the autocorrelation function of ith source where $*$ denotes the conjugate operator, σ^2 is the noise power of $n_m(t)$ and $\delta(\cdot)$ is the impulse function. It is noteworthy that we will ignore the noise term in (3) at $l = 0$ and $\tau = 0$ in the following development as σ^2 is assumed known *a priori* or accurately estimated [16].

Equations (3)–(5) show that the noise-free correlation sequence corresponds to the time series of harmonic sequences with harmonic frequencies given by ω_i, $\omega_i - \phi_i$ and $\omega_i + \phi_i$, respectively. Therefore, we can estimate the harmonic components by a subspace-based high-resolution estimation method.

For $l = 0, 1, 2, \ldots, N$, we define the following vectors with the use of (3)–(5):

$$\mathbf{X}(\tau) = [r_{(0,0)}(\tau), r_{(-1,1)}(\tau), \ldots, r_{(-N,N)}(\tau)]^T_{(N+1)\times 1} \tag{8}$$

$$\mathbf{Y}(\tau) = [r_{(-1,0)}(\tau), r_{(-2,1)}(\tau), \ldots, r_{(-N,N-1)}(\tau)]^T_{N\times 1} \tag{9}$$

$$\mathbf{Z}(\tau) = [r_{(1,0)}(\tau), r_{(0,1)}(\tau), \ldots, r_{(-N+1,N)}(\tau)]^T_{(N+1)\times 1} \tag{10}$$

where T denotes the transpose operator. Note that the dimension of $\mathbf{Y}(\tau)$ is different from those of $\mathbf{X}(\tau)$ and $\mathbf{Z}(\tau)$.

We can rewrite (8)–(10) in matrix form as:

$$\mathbf{X}(\tau) = \mathbf{A}_x(\omega_1, \omega_2, \ldots, \omega_P)\mathbf{R}_s(\tau) \tag{11}$$

$$\mathbf{Y}(\tau) = \mathbf{A}_y(\omega_1 - \phi_1, \omega_2 - \phi_2, \ldots, \omega_P - \phi_P)\mathbf{R}_s(\tau) \tag{12}$$

$$\mathbf{Z}(\tau) = \mathbf{A}_z(\omega_1 + \phi_1, \omega_2 + \phi_2, \ldots, \omega_P + \phi_P)\mathbf{R}_s(\tau) \tag{13}$$

where

$$\mathbf{R}_s(\tau) = [r_{s_1 s_1}(\tau), \ldots, r_{s_i s_i}(\tau), \ldots, r_{s_P s_P}(\tau)]^T \tag{14}$$

$$\mathbf{A}_x = \begin{pmatrix} 1 & \cdots & 1 \\ e^{-j2\omega_1} & \cdots & e^{-j2\omega_P} \\ \vdots & \vdots & \vdots \\ e^{-j2\omega_1 N} & \cdots & e^{-j2\omega_P N} \end{pmatrix}_{(N+1)\times P} \tag{15}$$

$$\mathbf{A}_y = \begin{pmatrix} e^{-j(\omega_1-\phi_1)} & \cdots & e^{-j(\omega_P-\phi_P)} \\ e^{-j3(\omega_1-\phi_1)} & \cdots & e^{-j3(\omega_P-\phi_P)} \\ \vdots & \vdots & \vdots \\ e^{-j(2N+1)(\omega_1-\phi_1)} & \cdots & e^{-j(2N+1)(\omega_P-\phi_P)} \end{pmatrix}_{N\times P} \tag{16}$$

$$\mathbf{A}_z = \begin{pmatrix} e^{-j(-1)(\omega_1+\phi_1)} & \cdots & e^{-j(-1)(\omega_P+\phi_P)} \\ e^{-j(\omega_1+\phi_1)} & \cdots & e^{-j(\omega_P+\phi_P)} \\ \vdots & \vdots & \vdots \\ e^{-j(2N-1)(\omega_1+\phi_1)} & \cdots & e^{-j(2N-1)(\omega_P+\phi_P)} \end{pmatrix}_{(N+1)\times P} \tag{17}$$

We sample again the correlation sequences

$$\{r_{(-l,l)}(\tau), r_{(-l-1,l)}(\tau), r_{(-l+1,l)}(\tau)\}$$

at K lags where K denotes the number of "pseudo-snapshots" [14, 15]. Let $\tau = 0, T_s, 2T_s, \ldots, (K-1)T_s$ where T_s represents the sample interval of the pseudo-snapshots which is chosen as an integral multiple of the original sample interval of the observed data $x_m(t)$. As a result, $(K-1)T_s$ is always smaller than the number of samples of the observed array data M. The value of K should satisfy $N < (K-1) \le M/T_s$ and $(K-1)T_s \le L$ is required to ensure $r_{s_i s_i}((K-1)T_s) \ne 0$ where L is the correlation length of the source signals.

We then obtain the following data matrices using the spatial-temporal samples,

$$\mathbf{R}_x = [\mathbf{X}(0T_s), \mathbf{X}(T_s), \mathbf{X}(2T_s), \ldots, \mathbf{X}((K-1)T_s)]_{(N+1)\times K} = \mathbf{A}_x \mathbf{R}_0 \quad (18)$$

$$\mathbf{R}_y = [\mathbf{Y}(0T_s), \mathbf{Y}(T_s), \mathbf{Y}(2T_s), \ldots, \mathbf{Y}((K-1)T_s)]_{N\times K} = \mathbf{A}_y \mathbf{R}_0 \quad (19)$$

$$\mathbf{R}_z = [\mathbf{Z}(0T_s), \mathbf{Z}(T_s), \mathbf{Z}(2T_s), \ldots, \mathbf{Z}((K-1)T_s)]_{(N+1)\times K} = \mathbf{A}_z \mathbf{R}_0 \quad (20)$$

where

$$\mathbf{R}_0 = [\mathbf{R}_s(0), \mathbf{R}_s(T_s), \ldots, \mathbf{R}_s((K-1)T_s)]_{P\times K} \quad (21)$$

Now we define

$$\mathbf{R}_{x1} = \mathbf{R}_x(1:N,:) \qquad \text{and} \qquad \mathbf{R}_{x2} = \mathbf{R}_x(2:(N+1),:) \quad (22)$$

where $\mathbf{R}_x(k:l,:)$ takes the k-th to l-th rows of $\mathbf{R}_x$. We have

$$\mathbf{R}_{x1} = \mathbf{A}_{x1} \mathbf{R}_s \qquad \text{and} \qquad \mathbf{R}_{x2} = \mathbf{A}_{x1} \mathbf{\Phi}_x \mathbf{R}_s \quad (23)$$

where

$$\mathbf{A}_{x1} = \mathbf{A}_x(1:N,:) \quad (24)$$

and

$$\mathbf{\Phi}_x = \begin{pmatrix} e^{-j2\omega_1} & 0 & \ldots & 0 \\ 0 & e^{-j2\omega_2} & \ldots & 0 \\ \vdots & \vdots & \ddots & \vdots \\ 0 & 0 & \ldots & e^{-j2\omega_P} \end{pmatrix} \quad (25)$$

It is assumed that the matrices $\mathbf{A}_x$ and $\mathbf{R}_0$ are of full rank. The full rank assumption of $\mathbf{A}_x$ is classical and is generally valid for real applications. In applications such as radar, sonar and wireless communications, the *a priori* knowledge of source signals is available and hence the condition that $\mathbf{R}_0$ is full rank can be satisfied [14, 15]. Following [15], we can easily obtain:

$$\mathbf{R}_1 \mathbf{A}_{x1} = \mathbf{A}_{x1} \mathbf{\Phi}_x \quad (26)$$

where $\mathbf{R}_1$ is calculated as

$$\mathbf{R}_1 = \mathbf{R}_{x2}[\mathbf{R}_{x1}]^{\#} \tag{27}$$

with $(\cdot)^{\#}$ denotes the pseudo-inverse of a matrix.

Similar to (21)–(23), we use (19)–(20) to obtain:

$$\mathbf{R}_2 \mathbf{A}_{y1} = \mathbf{A}_{y1} \boldsymbol{\Phi}_y \qquad \text{and} \qquad \mathbf{R}_3 \mathbf{A}_{z1} = \mathbf{A}_{z1} \boldsymbol{\Phi}_z \tag{28}$$

where

$$\mathbf{R}_2 = \mathbf{R}_y(2:N,:)[\mathbf{R}_y(1:(N-1),:)]^{\#} \tag{29}$$

$$\mathbf{R}_3 = \mathbf{R}_z(2:(N+1),:)[\mathbf{R}_z(1:N,:)]^{\#} \tag{30}$$

$$\mathbf{A}_{y1} = \mathbf{A}_y(1:(N-1),:) \qquad \text{and} \qquad \mathbf{A}_{z1} = \mathbf{A}_z(1:N,:) \tag{31}$$

$$\boldsymbol{\Phi}_y = \begin{pmatrix} e^{-j2(\omega_1-\phi_1)} & 0 & \cdots & 0 \\ 0 & e^{-j2(\omega_2-\phi_2)} & \cdots & 0 \\ \vdots & \vdots & \ddots & \vdots \\ 0 & 0 & \cdots & e^{-j2(\omega_P-\phi_P)} \end{pmatrix} \tag{32}$$

and

$$\boldsymbol{\Phi}_z = \begin{pmatrix} e^{-j2(\omega_1+\phi_1)} & 0 & \cdots & 0 \\ 0 & e^{-j2(\omega_2+\phi_2)} & \cdots & 0 \\ \vdots & \vdots & \ddots & \vdots \\ 0 & 0 & \cdots & e^{-j2(\omega_P+\phi_P)} \end{pmatrix} \tag{33}$$

Note that the dimensions of $\mathbf{R}_1, \mathbf{R}_2$ and $\mathbf{R}_3$ are $N \times N, (N-1) \times (N_1)$ and $N \times N$, respectively. As a result, the estimates of the matrices $\boldsymbol{\Phi}_x$, $\boldsymbol{\Phi}_y$, and $\boldsymbol{\Phi}_z$ can be given by the P nonzero eigenvalues from the eigenvalue decomposition of $\mathbf{R}_1$, $\mathbf{R}_2$, and $\mathbf{R}_3$, respectively. The angles and ranges estimates are easily computed by the diagonal elements of $\boldsymbol{\Phi}_x, \boldsymbol{\Phi}_y$, and $\boldsymbol{\Phi}_z$.

To estimate the ranges and angles of the sources, we first need to pair the elements of the three sets of parameters, namely, $\{\hat{\omega}_i\}$, $\{\hat{\omega}_i - \hat{\phi}_i\}$, and $\{\hat{\omega}_i + \hat{\phi}_i\}$ where $\hat{\omega}_i$ and $\hat{\phi}_i$ represent the estimate of ω_i and ϕ_i, respectively. This is achieved as follows [11]. For each $\hat{\omega}_i$, $1 \leq i \leq P$, its corresponding value of $\hat{\phi}_i$ is obtained as:

$$\hat{\phi}_i = \left[\left(\hat{\omega}_{l_0} + \hat{\phi}_{l_0} \right) - \left(\hat{\omega}_{k_0} - \hat{\phi}_{k_0} \right) \right] / 2 \tag{34}$$

where the indexes (k_0, l_0) are given by

$$(k_0, l_0) = \arg\min_{k,l} \left| \hat{\omega}_i - \left[\left(\hat{\omega}_k + \hat{\phi}_k \right) + \left(\hat{\omega}_l - \hat{\phi}_l \right) \right] / 2 \right| \tag{35}$$

From each pair of $(\hat{\omega}_i, \hat{\phi}_i)$, $i = 1, 2, \ldots, P$, the estimates of the DOA and range parameters, denoted by $\hat{\theta}_i$ and $\hat{r}_i$, respectively, are computed as

$$\hat{\theta}_i = \sin^{-1}\left(\frac{-\lambda\hat{\omega}_i}{2\pi d}\right) \tag{36}$$

$$\hat{r}_i = \frac{\pi d^2 \cos^2\left(\hat{\theta}_i\right)}{\lambda\hat{\phi}_i} \tag{37}$$

The procedure of the proposed algorithm is summarized as

- Compute the estimates of $r_{(-l,l)}(\tau)$, $r_{(-l-1,l)}(\tau)$ and $r_{(-l+1,l)}(\tau)$ in (3)–(5) with removing the noise term in (3), and then construct $\mathbf{X}(\tau)$, $\mathbf{Y}(\tau)$, $\mathbf{Z}(\tau)$ using (8)–(10).
- Construct $\mathbf{R}_x$, $\mathbf{R}_y$, $\mathbf{R}_z$ according to (18)–(20).
- Compute $\mathbf{R}_1, \mathbf{R}_2$ and $\mathbf{R}_3$ using (27), (29) and (30).
- Perform eigenvalue decomposition of $\mathbf{R}_i, i = 1, 2, 3$, to obtain the corresponding eigenvalues, and then the parameter estimates, $\hat{\omega}_i$, $\hat{\omega}_i - \hat{\phi}_i$ and $\hat{\omega}_i + \hat{\phi}_i$, are calculated with the use of the phase angles of the corresponding eigenvalues.
- Pair the estimated parameters $\{\hat{\omega}_i, \hat{\omega}_i - \hat{\phi}_i, \hat{\omega}_i + \hat{\phi}_i\}$ using (34) and (35) and then get $(\hat{\omega}_i, \hat{\phi}_i)$.
- Compute the source location parameters, $\hat{\theta}_i$ and $\hat{r}_i$, $i = 1, 2, \ldots, P$, using (36) and (37).

Finally, it is helpful to compare the computational load of the proposed method with other methods not requiring searches. In the ESPRIT-like method [10], multiplications are needed in calculating four cumulant matrices and in performing the eigen-decompositions, which correspond to a complexity of $36N^2M + o((3N)^3) + o(P^3)$. Consider the dominant operations in the proposed and WLP methods, namely, multiplications involved in calculating the correlation sequences, performing the eigenvalue decompositions and additional weighting matrix inverses in the WLP method. The latter complexity is $3NM + o((P + 1)^3) + o((2N + 1 - P)^3)$ while that of the proposed algorithm is $3NM + o(N^3)$. Clearly, the computational load of the ESPRIT-like method is much larger than those of the other two methods. Since $P \le N$ is assumed in the proposed and WLP methods and $(2N + 1 - P) > P$, the former is also computationally simpler than the latter even in the case of using only one iteration. As an illustration, for $N = 3$ and $P = 2$, the proposed algorithm requires $o(27)$ computations in performing the eigen-decomposition while the complexities of the WLP and ESPRIT-like methods are $o(125)$ and $o(729)$, respectively.

4. SIMULATION RESULTS

A set of computer simulations is carried out to evaluate the performance of the proposed method. We consider a uniform linear array of $n = 2N + 1$ sensors with inter-element spacing of $d = \lambda/4$. All the sensor noise components $\{n_m(t)\}$ are zero-mean white Gaussian processes with identical powers. Both Gaussian and non-Gaussian signal sources are investigated. The performance is measured by the root mean square error (RMSE).

In the first experiment, there are $n = 7$ sensors or $N = 3$. Two non-Gaussian signal sources with equal powers, which are of the forms of $s_1(t) = e^{j(0.2\pi t + \varphi_1)}$ and $s_2(t) = e^{j(0.4\pi t + \varphi_2)}$ where $\{\varphi_i\}$ are independent and are uniformly distributed in $[0, 2\pi]$, are impinging on this array. The first source is located at $\theta_1 = 40°$ with a range of $r_1 = 5\lambda$, and the second is located at $\theta_2 = 20°$ with $r_2 = 1.5\lambda$. The number of samples is set to $M = 20$ and the number of pseudo-snapshots is $K = 10$ with $T_s = 2$. All results provided are averages of 100 independent runs. The RMSEs for the DOA and range estimates of the two sources are shown in Figures 2 and 3. For comparison, the results using the ESPRIT-like algorithm [10] as well as the WLP method [12] are also shown. We can see that the estimation accuracy of the proposed method is comparable to that of the WLP method, but it is much higher than that of ESPRIT-like method over all signal-to-noise ratio (SNR) conditions. Note that the performance of DOA estimation is similar for both sources while the RMSE of the range estimate for $s_2(t)$ is much lower than that of $s_1(t)$ because the second source is close to the array while the first source is far from it, and this agrees with the findings in [13].
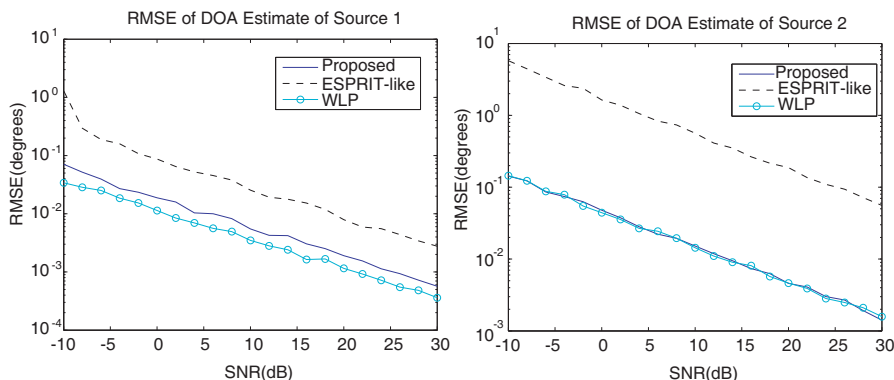
Figure 2. RMSEs of estimated DOA's versus input SNR.
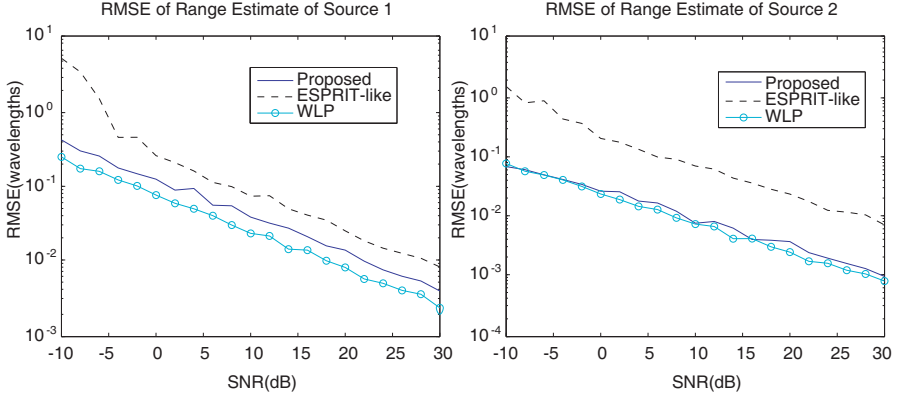
Figure 3. RMSEs of estimated ranges versus input SNR.
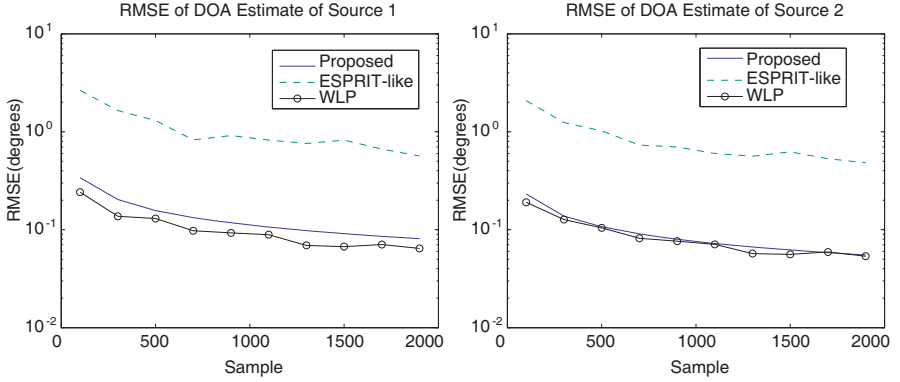
Figure 4. RMSEs of estimated DOA's versus M.

In the second experiment, the input SNR of the two non-Gaussian signal sources is assigned as $\text{SNR} = 5\,\text{dB}$ and we vary M from 100 to 2000, with the corresponding number of pseudo-snapshots is set to $K = M/2$. The results are based on 100 independent runs. The other parameter settings are same as those in the first experiment. It is seen from Figure 4 that the performance of the proposed method is superior to that of ESPRIT-like method [10], especially in the case of small number of snapshots, because the latter is based on the higher-order cumulants and larger number of samples are required for their accurate estimation. On the other hand, we observe that the performance of the proposed method is still close to that of the WLP method for different values of M.

In the third experiment, we consider two equal-power non-Gaussian signals impinging on an array of 9 sensors with $\mathrm{SNR} = 20\,\mathrm{dB}$, $M = 50$ and $K = 25$. The first source position is characterized by $(40°, 1.5\lambda)$ while the DOA of the second source is fixed at $20°$ with its range varies from 5λ to 20λ. 100 independent runs are conducted for each range parameter and the results for the DOA estimates are shown in Figure 5. We see that the performance of the proposed and WLP methods is much better than that of ESPRIT-like method for different ranges of the second source.
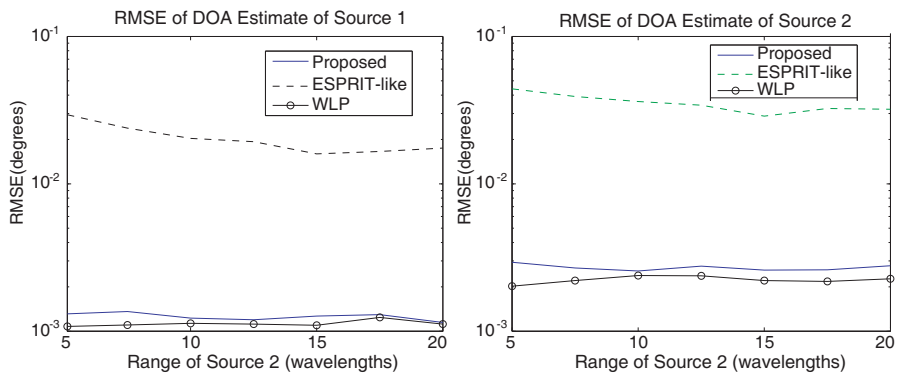

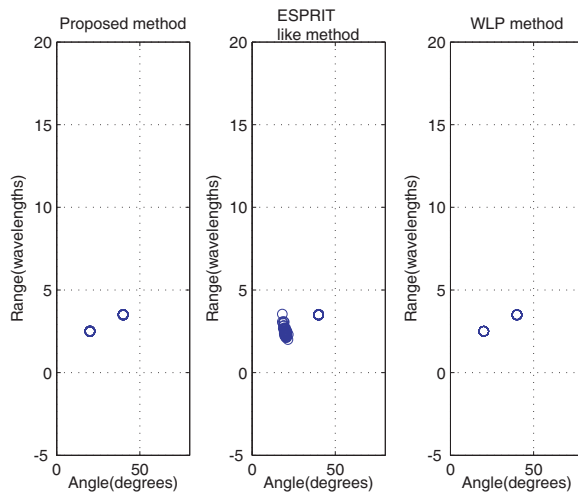**Figure 5.** RMSEs of estimated DOA's versus range of second source.

Figure 6. Estimated ranges and DOA's for two non-Gaussian sources with unequal powers.

In the fourth experiment, the positions of the first and second non-Gaussian sources are characterized by $(40°, 3.5\lambda)$ and $(20°, 2.5\lambda)$, respectively, and they have different input SNR values, namely, 20 dB and 10 dB. We assign $n = 11$, $M = 50$ and $K = 25$. The results based on 50 independent runs are shown in Figure 6. We observe that the proposed and WLS methods are comparable and their performance is better than that of the ESPRIT-like method when the two sources have unequal noise powers.

In the fifth experiment, we consider that there are three non-Gaussian uncorrelated signal sources impinging on the received array. The first and second source signals are same as before while $s_3(t) = e^{j(0.8\pi t + \varphi_3)}$, and the position parameters are $(60°, 3.5\lambda)$, $(40°, 2.5\lambda)$, $(20°, 1.5\lambda)$, respectively. The input SNRs of all received signals are equal to 20 dB while $n = 15$, $M = 100$ and $K = 50$. It is shown in Figure 7 that the performance of the proposed method and the WLS scheme is comparable and they are superior to the ESPRIT-like method, particularly for the range estimates [13].

In the last experiment, we consider two uncorrelated colored Gaussian signal sources whose positions are parameterized by $(40°, 0.5\lambda)$ and $(20°, 2.5\lambda)$. The input SNRs of the two signals are both equal to 20 dB while $n = 11$, $M = 100$ and $K = 50$. The results based on 50 independent runs are shown in Figure 8. As mentioned
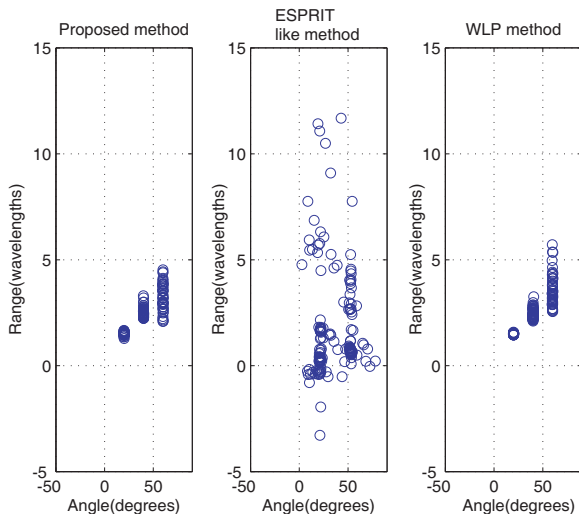
Figure 7. Estimated ranges and DOA's for three non-Gaussian sources with equal powers.

in Section 1, the ESPRIT-like method which utilizes the fourth-order cumulants fails to resolve the two Gaussian signal sources. On the other hand, it is seen that the two methods using second-order statistics can still give accurate estimates of ranges and angles for colored Gaussian signal sources.
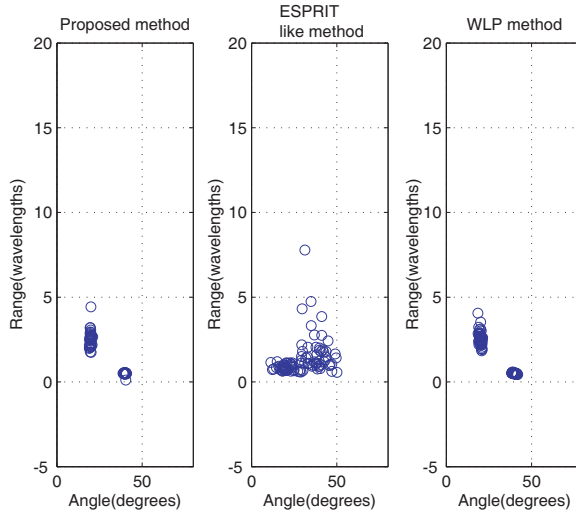
Figure 8. Estimated ranges and DOA's for two Gaussian signal sources with equal powers.

5. CONCLUSION

In this paper, a novel subspace method based on spatial-temporal structure is presented for localization of multiple near-field sources. The proposed algorithm only uses second-order statistics and requires a simple pair-matching method in the case of multiple near-field sources. Compared with several existing methods without search operation, the proposed method is more computationally efficient. It is shown that the estimation accuracy of the proposed method is comparable to the weighted linear prediction scheme and is superior to the ESPRIT-like method. As a future work, we will produce the performance analysis of the parameter estimates.

ACKNOWLEDGMENT

REFERENCES

1. Krim, H. and M. Viberg, "Two decades of array signal processing research: The parametric approach," *IEEE Signal Processing Magazine*, Vol. 13, No. 4, 67–94, July 1996.
2. Kim, J. H., I. S. Yang, K. M. Kim, and W. T. Oh, "Passive ranging sonar based on multi-beam towed array," *Proc. IEEE Oceans*, Vol. 3, 1495–1499, September 2000.
3. Swindlelhurst, A. L. and T. Kailath, "Passive direction of arrival and range estimation for near-field sources," *IEEE Spec. Est. and Mod. Workshop*, 123–128, 1988.
4. Huang, Y. D. and M. Barkat, "Near-field multiple sources localization by passive sensor array," *IEEE Trans. Antennas Propag.*, Vol. 39, 968–975, July 1991.
5. Jeffers, R., K. L. Bell, and H. L. Van Trees, "Broadband passive range estimation using MUSIC," *Proc. IEEE Int. Conf. Acoust. Speech, Signal Processing*, Vol. 3, 2920–2922, Orlando, Florida, USA, May 2002.
6. Starer, D. and A. Nehorai, "Path-following algorithm for passive localization of near-field sources," *5th ASSP Workshop on Spectrum Estimation and Modeling*, 322–326, October 1990.
7. Lee, J. H., C. M. Lee, and K. K. Lee, "A modified path-following algorithm using a known algebraic path," *IEEE Trans. Signal Processing*, Vol. 47, 1407–2409, May 1999.
8. Lee, C. M., K. S. Yoon, and K. K. Lee, "Efficient algorithm for localising 3-D narrowband multiple sources," *IEE Proc. Radar, Sonar Navig.*, Vol. 148, 23–26, Febuary 2001.
9. Weiss, A. J. and B. Friedlander, "Range and bearing estimation using polynomial rooting," *IEEE J. Ocean. Engr.*, Vol. 18, 130–137, April 1993.
10. Challa, R. N. and S. Shamsunder, "Higher-order subspace based algorithms for passive localization of near-field sources," *Proc. 29th Asilomar Conf. Signals System Computer*, 777–781, Pacific Grove, CA, October 1995.

11. Grosicki, E. and K. Abed-Meraim, "A weighted linear prediction method for near-field source localization," *Proc. IEEE Int. Conf. Acoust. Speech, Signal Processing*, 2957–2960, Orlando, Florida, USA, May 2002.

12. Grosicki, E., K. Abed-Meraim, and Y. Hua, "A weighted linear prediction method for near-field source localization," *IEEE Trans. Signal Process.*, Vol. 53, 3651–3660, October 2005.

13. Yuen, N. and B. Friedlander, "Performance analysis of higher-order ESPRIT for localization of near-field sources," *IEEE Trans. Signal Processing*, Vol. 46, No. 3, 709–719, March 1998.

14. Jin, L., Q.-Y. Yin, and B.-F. Jiang, "Direction finding of wideband signals via spatial-temporal processing in wireless communications," *Prof. IEEE International Symposium on Circuits and Systems*, Vol. 2, 81–84, Geneva, Switzerland, May 2000.

15. Deng, K., Q. Yin, L. Ding, and Z. Zhao, "Blind channel estimator for V-BLAST coded DS-CDMA system in frequency selective fading environment," *Proc. IEEE VTC'2003 Fall*, Orlando, USA, 458–462, 2003.

16. Stoica, P. and T. Soderatrom, "On estimating the noise power in array processing," *Signal Processing*, Vol. 26, No. 2, 205–220, 1992.